Supporting Information

Improved ON/OFF Ratio in Interface-Type Memristors with Ion Irradiation-Induced Large Schottky Barrier for Neuromorphic Computing

Ruowei Wang[1], Jie Su[2*], Yong Liu[3*], Minghui Xu[2], Minghao Zhang[1], Pengshun Shan[2], Weijin Kong[1*], Yuyi Li[2], Hao Wu[1], Tao Liu[2*]

[1] College of Physics Science, Qingdao University, Qingdao 266071, People's Republic of China

[2] College of Electronic and Information Engineering, Qingdao University, Qingdao 266071, People's Republic of China

[3] Shandong Provincial Key Laboratory of Nuclear Science, Nuclear Energy Technology and Comprehensive Utilization, School of Nuclear Science, Energy and Power Engineering, Shandong University, Jinan 250061, People's Republic of China

* Corresponding authors. E-mail addresses: jsu@qdu.edu.cn (J. Su), yongliu@sdu.edu.cn (Y. Liu), kwjsd@163.com (W. Kong), liutao@qdu.edu.cn (T. Liu).

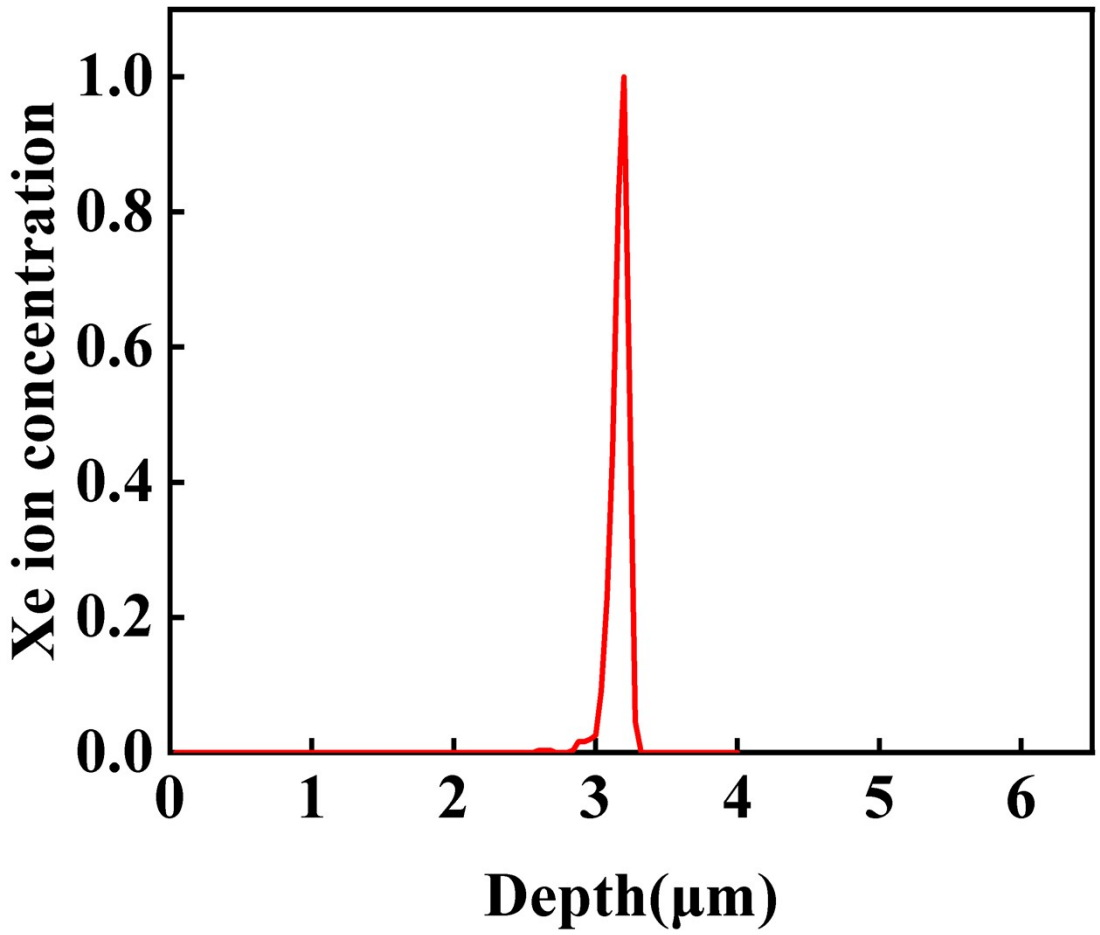

Figure. S1 The normalized curve of ion concentration distribution as a function of depth.

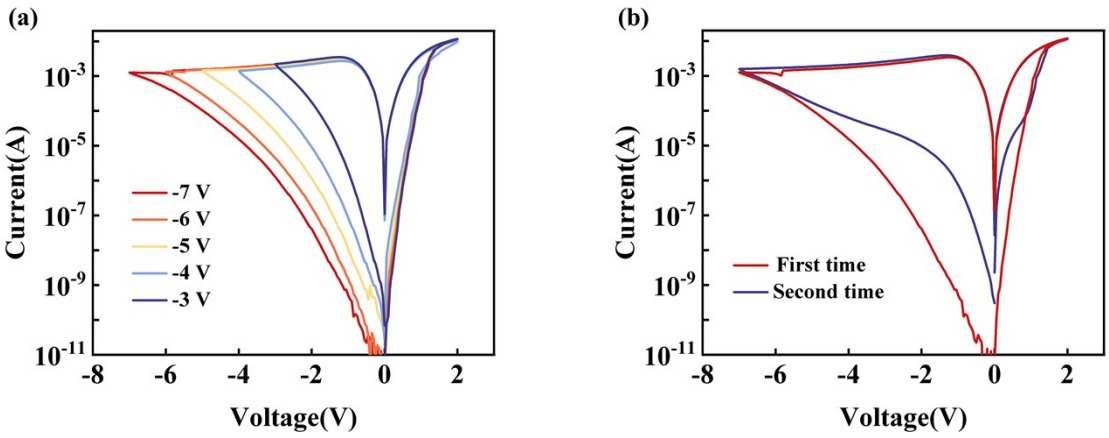

Figure. S2. (a) The *I-V* curves under different negative voltages. (b) *I-V* curves for the initial and subsequent sweeps at -7 V.

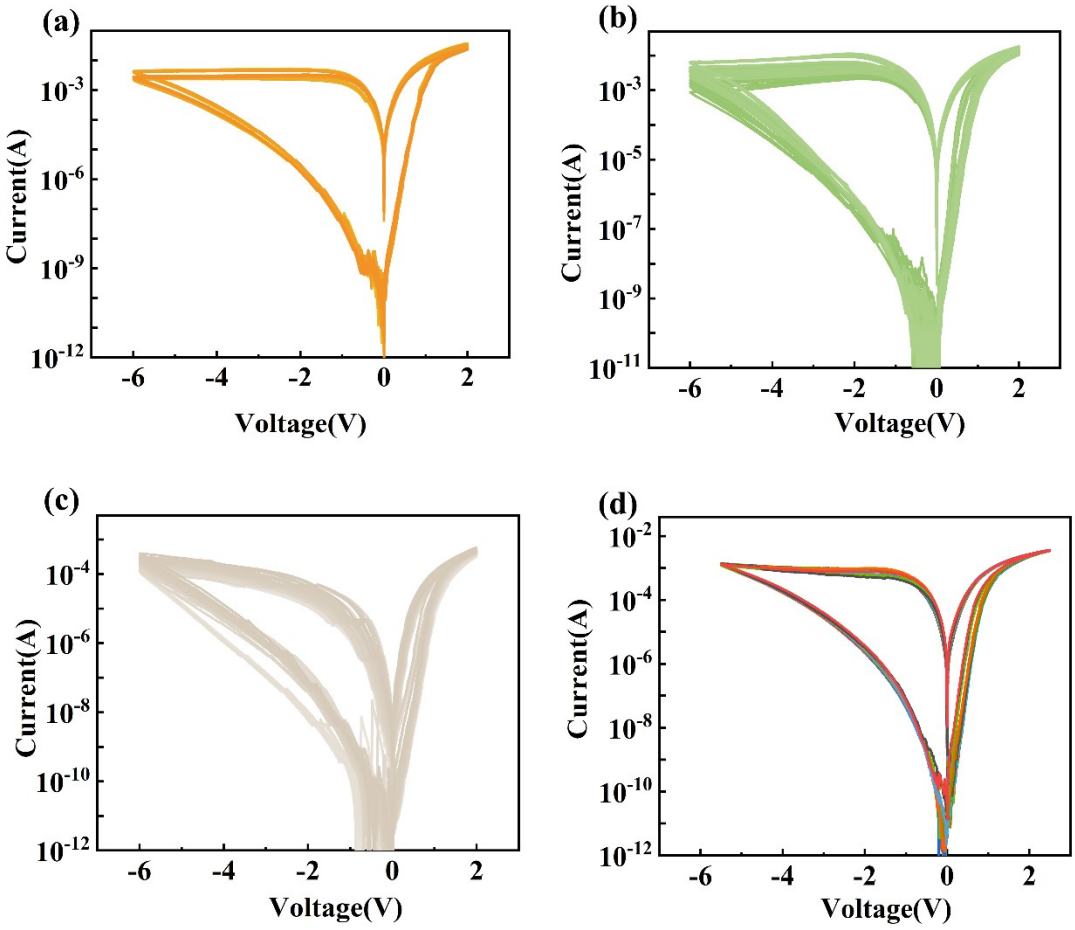

Figure. S3. 100 *I-V* cycle curves of (a) D_0, (b) D_1, (c) D_2, and (d)D_3.

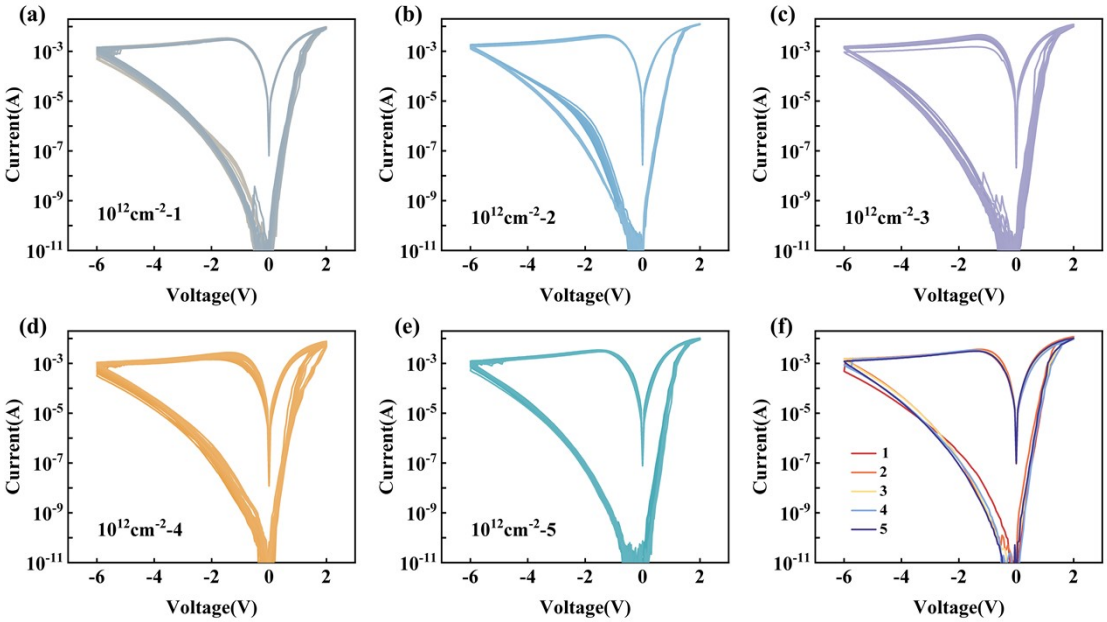

Figure. S4. The *I-V* curve cycles of device (a) 1, (b) 2, (c) 3, (d) 4, (e) 5. (f) Comparison of *I-V* curves of five devices.

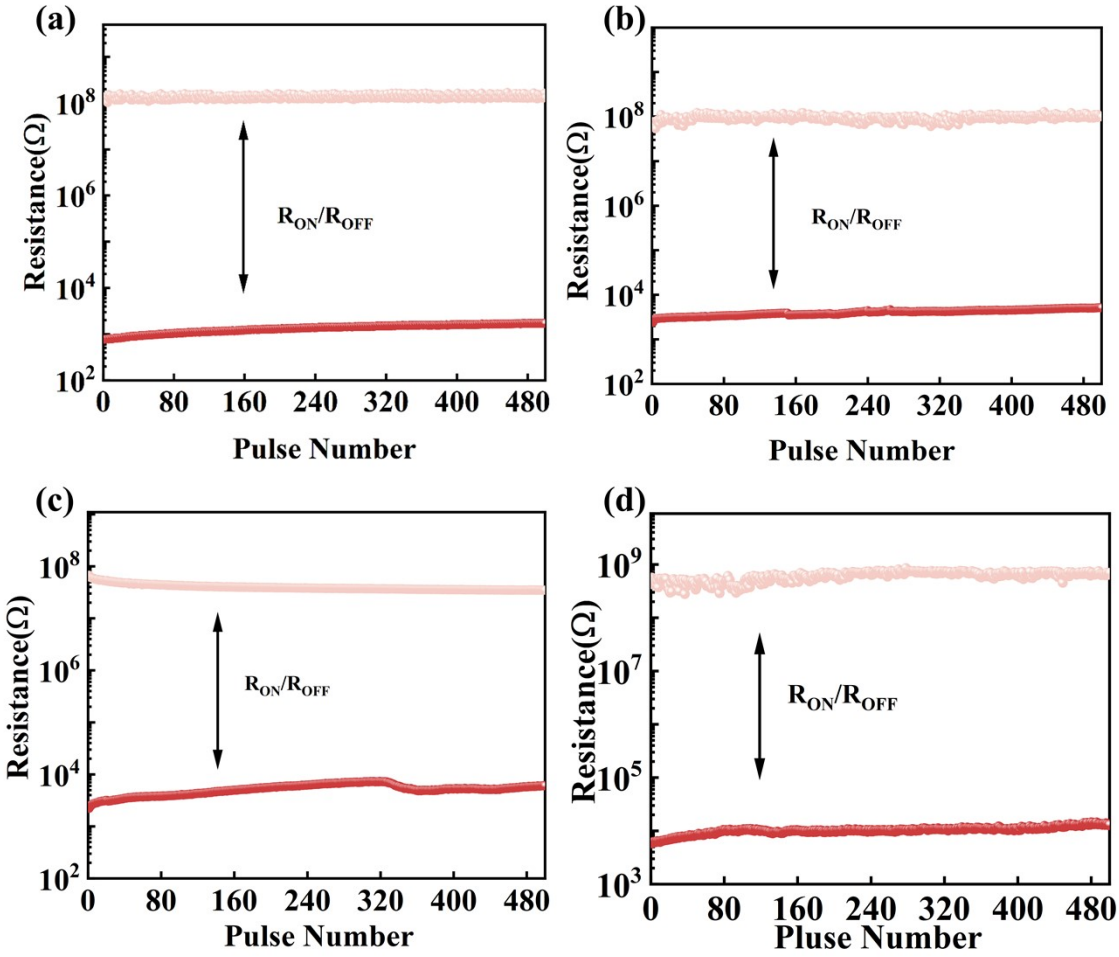

Figure. S5. The on/off radio of (a) D_0, (b) D_1, (c) D_2, and (d)D_3.

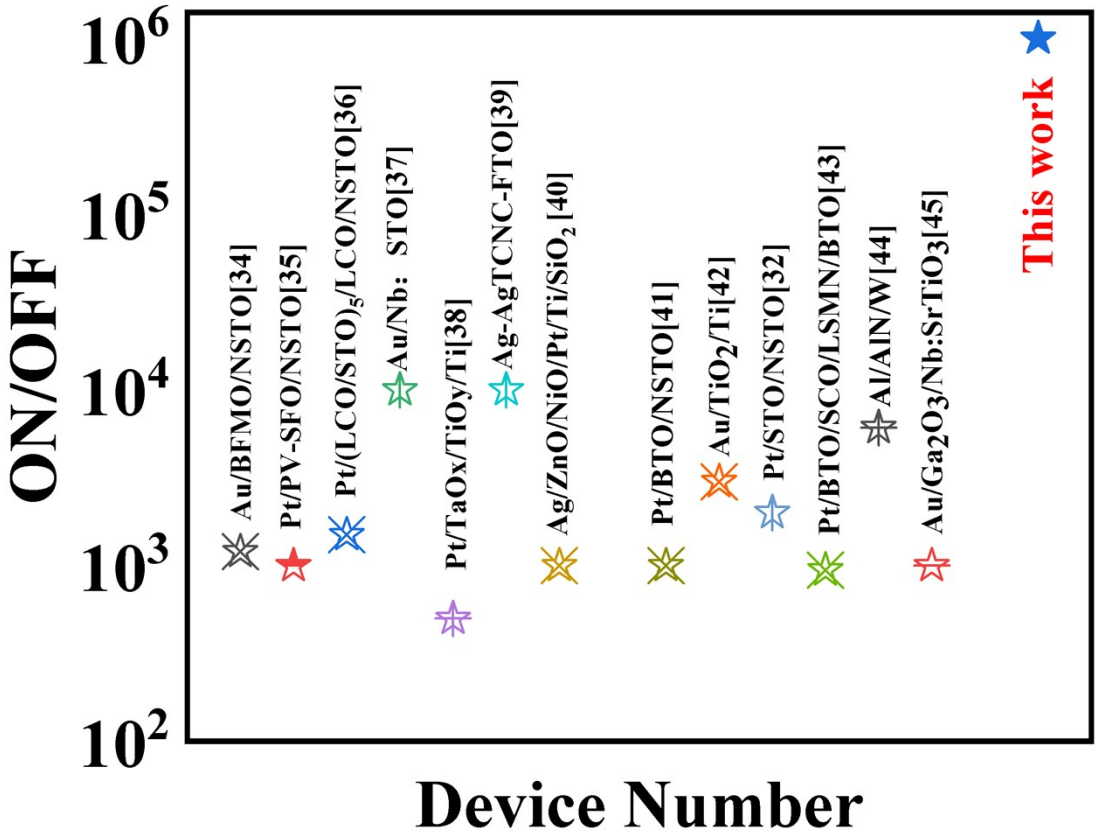

Figure. S6. Comparison of switching ratio between D_4 device and other memristors.

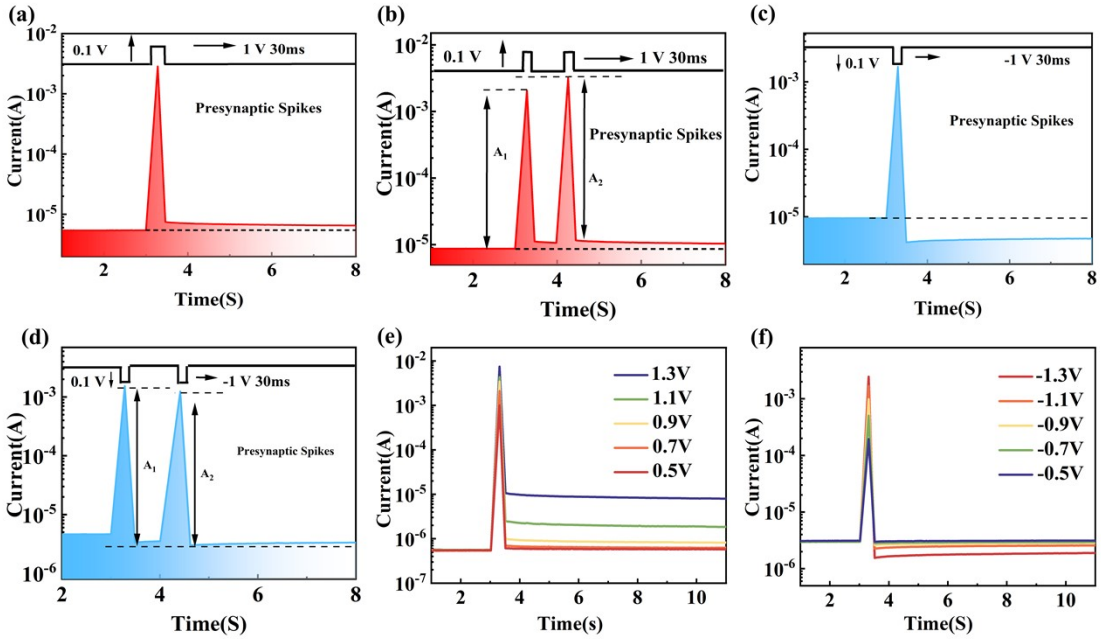

Figure.S7. EPSC stimulated with (a) a single and (b) two positive pulse amplitudes on D_4. IPSC stimulated with (c) a single and (d) two negative pulse amplitudes on D_4. (e) EPSC and (f) IPSC stimulated with different pulse amplitudes.

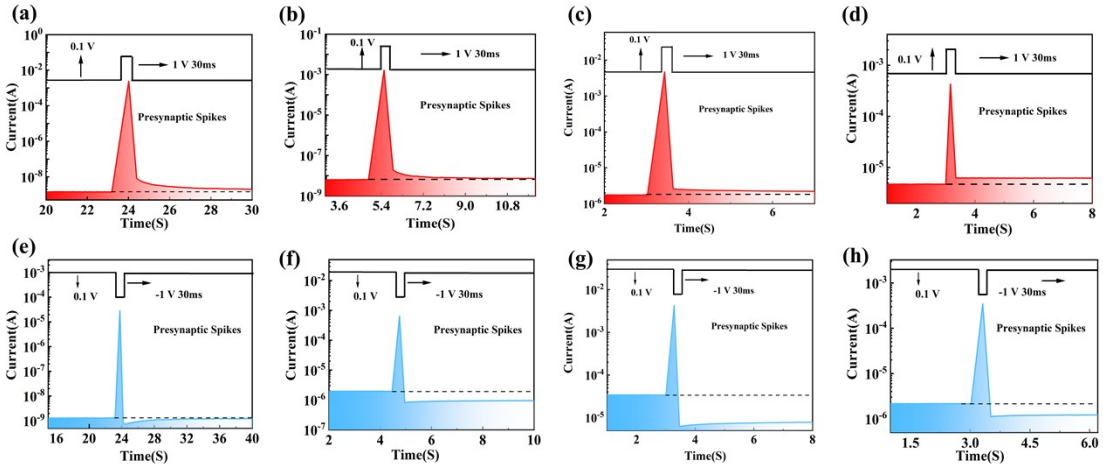

Figure. S8. EPSC stimulated with a single positive pulse amplitude on (a) D_0, (b) D_1, (c) D_2, and (d) D_3. IPSC stimulated with a single negative pulse amplitude on (e) D_0, (f) D_1, (g) D_2, and (h) D_3.

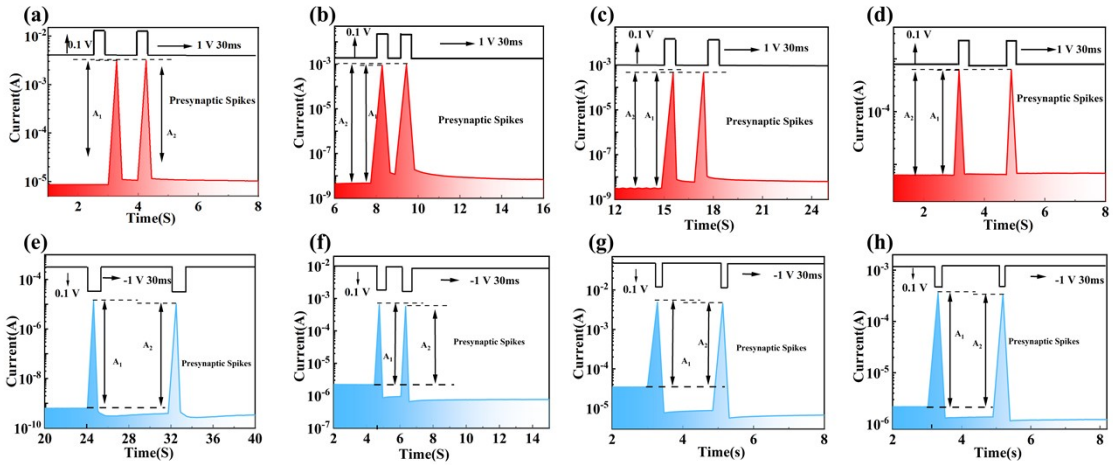

Figure. S9. EPSC stimulated with two positive pulse amplitudes on (a) D_0, (b) D_1, (c) D_2, and (d) D_3. IPSC stimulated with two negative pulse amplitudes on (e) D_0, (f) D_1, (g) D_2, and (h) D_3.

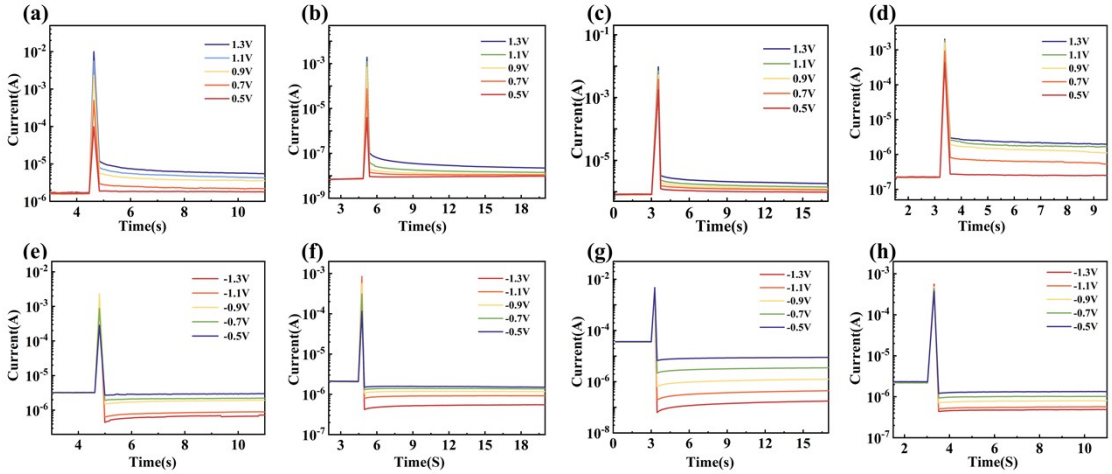

Figure. S10. EPSC stimulated with different pulse amplitudes on (a) D_0, (b) D_1, (c) D_2, and (d) D_3. IPSC stimulated with different pulse amplitudes on (a) D_0, (b) D_1, (c) D_2, and (d) D_3.

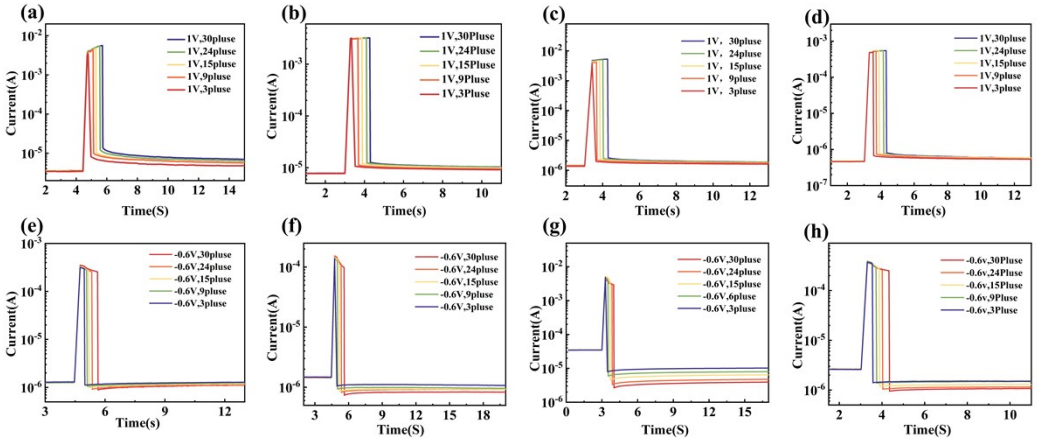

Figure. S11. EPSC stimulated with different numbers of pulses on (a) D_0, (b) D_1, (c) D_2, and (d) D_3. IPSC stimulated with different numbers of pulses on (a) D_0, (b) D_1, (c) D_2, and (d) D_3.

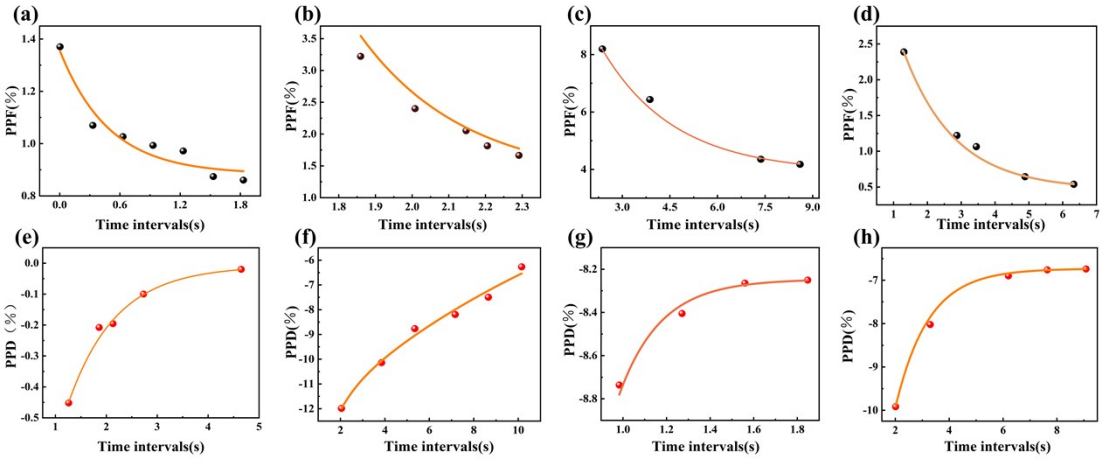

Figure. S12. PPF index as a function of Δt with (a) D_0, (b) D_1, (c) D_2, and (d) D_3. PPD index as a function of Δt with (a) D_0, (b) D_1, (c) D2, and (d) D_3.

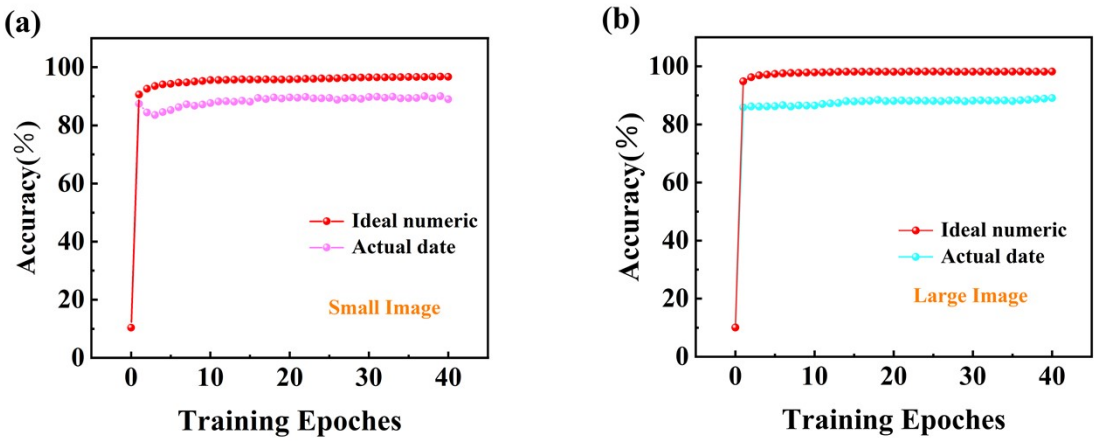

Figure. S13. (a)Training accuracy to small image of the D_4. (b) Accuracy after adding noise to large image of D_4.

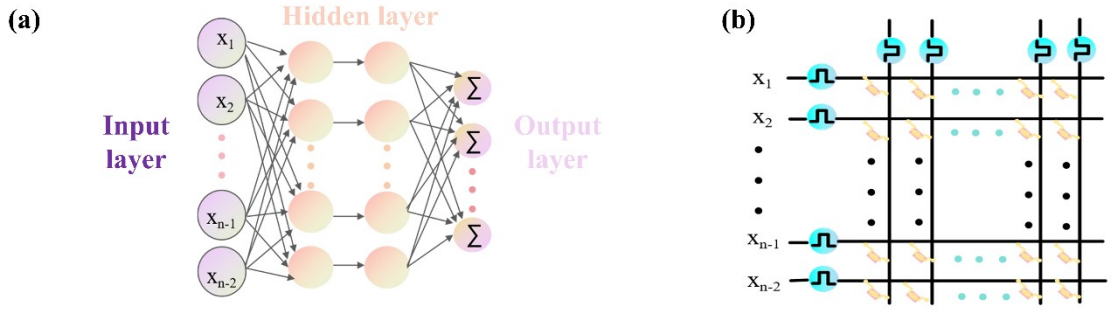

Figure. S14. Schematic diagram of (a) neural network and (b) crossbar neural nucleus with memristor as nodes.